

A Rapid and Efficient Way to Dynamic Creation of Cross-Reactive Sensor Arrays Based on Ionic Liquids

Wei Zhu,^[a] Weina Li,^[a] Haowei Yang,^[a] Yin Jiang,^[a] Chen Wang,^[a] Yu Chen,^[b] and Guangtao Li^{*[a]}

Abstract: Based on the simple counterion exchange of ionic liquids, a rapid, facile, and efficient strategy to create a cross-reactive sensor array with a dynamic tunable feature was developed, and exemplified by the construction of a sensor array for the identification and classification of nitroaromatics and explosives mimics. To achieve a good sensing system with fast response, good sensitivity, and low detection limit, the synthesized ionic liquid receptors were tethered onto a silica matrix with a macro-mesoporous hierarchical structure. Through the facile anion exchange approach, abundant ionic-

liquid-based individual receptors with diversiform properties, such as different micro-environments, diverse molecular interactions, and distinctive physico-chemical properties, were easily and quickly synthesized to generate a distinct fingerprint of explosives for pattern recognition. The reversible anion exchange ability further endowed the sensor array with a dynamic tunable feature as well as good controllability

and practicality for real-world application. With the assistance of statistical analysis, such as principal component analysis (PCA) and linear discrimination analysis (LDA), an optimized-size array with a good resolution was rationally established from a large number of IL-based receptors. The performed experiments suggested that the ionic-liquid-based sensing protocol is a general and powerful strategy for creating a cross-reactive sensor array that could find a wide range of applications for sensing various analytes or complex mixtures.

Keywords: cross-reactive • dynamic creation • explosive detection • ionic liquids • sensors

Introduction

Inspired by the mammalian olfactory system, a cross-reactive sensor array has become a powerful tool for the identification and classification of analytes based on the formation of distinct patterns generated through the interaction with non-specific, but semi-selective receptors.^[1] Up to now, there are numerous examples in the literature on sensor arrays for differential sensing of various analytes by using various synthetic receptors.^[2] For example, Anslyn et al. exploited diversiform synthetic receptors, which are composed of combinatorial peptidic arms, various metal ions, and numerous indicators, to rapidly construct sensor arrays.^[3] Shimizu et al. demonstrated the utility of molecularly imprinting processes for effectively creating differential receptors in arrays.^[4] Anzenbacher et al. described the rational design of different classes of fluorescent receptors to create differential sensing

protocols that nicely classify various metal ions.^[5] And quite recently, the combinational strategy for creating synthetic receptors or using gold nanoparticles and conjugated polymers as sensing elements had been separately reported by Hamilton et al. and Rotello et al.^[6] In another approaches, Severin and Buryak^[7] highlighted the remarkable power of differential sensing by combining simple transition metals with dyes and also Suslick et al. targeted the optoelectronic nose by using a series of cross-responsive dye molecules.^[8]

Nevertheless, there still exist some factors that limit further applications of the sensor array format. One of the major challenges besetting the development of an array-based sensing protocol is the requirement of rapidly and efficiently collecting/synthesizing a large number of receptors with abundant diversities.^[9] This is the crucial point for creating high-dispersion sensor arrays. When an array owns a high-dispersion property, it not only offers a high level of dimensionality, which is beneficial to improve the discrimination capability, but this also helps to obtain a high resolution sensor array.^[5] However, the preparation of the individual receptor is always a time- and resource-intensive process and the creation of an array of numerous receptors by rationally designing would multiply the difficulties.^[10] In this context, the design and development of a general, rapid, and efficient way to create receptors with abundant diversities in a cross-reactive sensor array is highly desirable.

Another limitation of the array-based sensing protocol is the lack of a dynamic tunable feature, which would be bene-

[a] W. Zhu, W. Li, H. Yang, Y. Jiang, C. Wang, Prof. Dr. G. Li
Department of Chemistry, Tsinghua University
Beijing, 100084 (P. R. China)
E-mail: lgt@mail.tsinghua.edu.cn

[b] Prof. Dr. Y. Chen
Department State Key Laboratory of Heavy Oil Processing
College of Chemical Engineering
China University of Petroleum
Beijing, 102249 (P.R. China)

Supporting information for this article is available on the WWW under <http://dx.doi.org/10.1002/chem.201300789>.

ficial for the prescreening of individual receptors to efficiently achieve the ultimate application of a sensor array for the identification and quantification of the target analytes. This dynamic feature not only focuses on dynamically tuning the individual receptors in the aspects of their properties and thus their sensing capabilities, but also the overall characteristic and performance of the array. As mentioned above, currently, numerous methods have been developed to synthesize a large number of receptors for sensor array construction. However, once these individual receptors have been synthesized, it is not easy to further adjust their properties and sensing behaviors. As a result, further optimizing the characteristic and performance of the created array would often need to rebuild the whole array. Obviously, this reconstruction would be a time-consuming and labor-intensive process. Thus, for an ideal sensor array, the introduction of the dynamic tunable feature would endow the array with better controllability and practicality for real-world application.

Ionic liquids (ILs), a class of compounds consisting of organic cations and anions, exhibit a series of unique properties including negligible vapor pressure, high ionic conductivity, a wide electrochemical window, and in particular, a facile ion exchange capability.^[11] By virtue of simple exchange of the counterion, the IL-based moiety would process abundant functionalities, different microenvironments (the local hydrophilicity and hydrophobicity), and diverse molecular interactions as well as distinctive physicochemical properties.^[12] These distinct properties and easy synthesis makes ILs ideal candidates for sensing application. So far, there are some reports on the creation of molecular receptors by just simply utilizing different ionic liquids.^[13] However, the exploration of the excellent counterion exchange capability of ILs for a rapid, efficient, and dynamic synthesis of diversiform synthetic receptors for the creation of sensor array has not been reported.

Herein, based on the unique counterion exchange property of ionic liquids, we presented a new strategy for rapidly and efficiently creating cross-reactive sensor arrays with dynamic tunable feature. To achieve a good sensing system with a fast response, good sensitivity, and low detection limit, the synthesized IL receptors were tethered onto a silica matrix with a macro-mesoporous hierarchical structure. As a demonstration, an ionic liquid with a fluorescent phenanthro[9,10-d]imidazolium (PAI) cation core and I⁻ as counterion was synthesized as a primary sensor element (Scheme 1), in which the cationic part acted as a core-signaling unit, and the described strategy was exemplified by the formation of a sensor array for nitroaromatics and explosives mimics identification and classification. It was found that the LUMO–HOMO energies, the excitation and emission spectra, the fluorescent lifetimes as well as the sensing capability of the synthesized IL could be significantly influenced and tuned by coupling different counterions, indicating that from one single IL sensor element a big sensor element pool with rich diversities could be conceivably created by a simple exchange process of the counterions. Moreover,

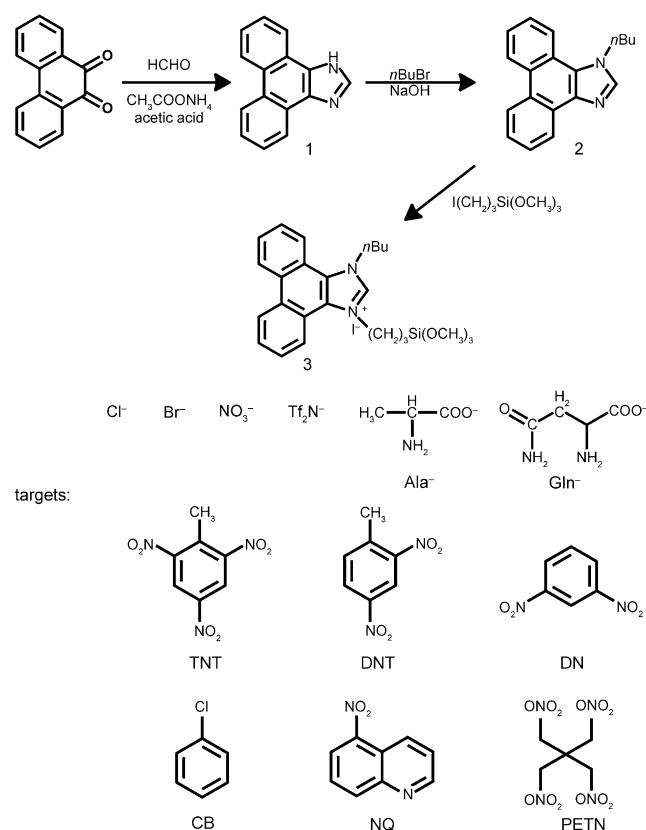
the reversible counterion exchange capability of ILs also provides a huge room and useful means to post-modify the sensing properties of an individual element for further correcting or optimizing the sensing performance of the formed sensor array, and endows the array with a desirable dynamic tunable feature. Indeed, a series of sensor elements was facilely produced by the exchange of the anion of the synthesized fluorescent ionic liquid with six different counterions such as Cl⁻, NO₃⁻, and Tf₂N⁻ (Tf = triflate) ions, and used as an array for nitroaromatics and explosives mimics detection and discrimination. The described dynamic tunable feature allows a rapid and efficient optimization of the formed array. Finally, based on the evaluation by using statistical analysis such as principal component analysis (PCA) and linear discrimination analysis (LDA), a cross-reactive sensor array with good discrimination ability and a high resolution was established.

Results and Discussion

Creation of the IL-based sensing elements with numerous diversities: A three-step approach was employed to synthesize the ionic-liquid-functionalized silane, as shown in Scheme 1. To achieve a good sensing system with a fast response, good sensitivity, and low detection limit, the synthesized fluorescent IL sensing element was tethered onto a silica matrix with a macro-mesoporous structure.^[14] Figure 1A shows the well-defined inverse replication of the formed polystyrene (PS) colloidal crystal arrays on a glass substrate (Figure S1 in the Supporting Information). The macropore size is about 180 nm with a wall thickness of 20 nm. XRD pattern displays a broad diffraction peak at 0.82°, which is typical for a worm-like mesostructure (Figure 1C), which was confirmed by TEM measurement (Figure 1B). Clearly, the mesochannels are distributed within the walls of the 3D-ordered macroporous silica and connect the adjacent macropores, which would facilitate the rapid diffusion of analyte molecules. The data of the Brunauer–Emmett–Teller (BET) surface area (198 m²g⁻¹) and the pore size (10 nm) from N₂ adsorption–desorption measurements further confirmed the hierarchical pore structure of the prepared silica films.

The correct incorporation of the synthesized ionic liquid into the silica matrix was proven by fluorescence measurement and FTIR spectroscopy. As shown in Figure 1D, the characteristic emission peaks of the PAI cation core in the silica film at wavelengths of $\lambda = 345, 360,$ and 389 nm were observable comparable to those of the IL monomer in ethanol solution (Figure S2 in the Supporting Information). Also the characteristic FTIR absorptions at $\tilde{\nu} = 3061, 3025, 1602,$ and 1581 cm⁻¹ confirmed the presence of the used ionic liquid moieties in the silica films (Figure S3a in the Supporting Information).

The anion exchange possibility of the immobilized IL moieties in silica films was firstly examined by soaking for 2 h. In our case, NaCl, NaBr, NaNO₃, NaPF₆, and LiTf₂N



Scheme 1. Top) Three-step approach to synthesize the PAI-based ionic liquid silane core for the counterion exchange. Middle) Six different anions used to create diversiform sensing elements for a sensor array construction. Bottom) Structure of the six nitroaromatics and explosives mimics for identification and classification. TNT = trinitrotoluol, DNT = dinitrotoluol, DN = dinitrobenzene, CB = chlorobenzene, NQ = nitroquinoline, PETN = pentaerythritol tetranitrate.

were used. As shown in Figure S3 in the Supporting Information, the characteristic FTIR absorptions of the corresponding anions appeared at $\tilde{\nu}$ = 1385, 1356, and 1681 cm⁻¹ separately, confirming the successful introduction of the different anionic groups. In consistent with the FTIR results, the change in the contact angle on the resulting silica films further proved the occurrence of the counterion exchange (Figure S4 in the Supporting Information). These results clearly indicate that the unique counterion exchange feature of ILs allows for rapidly accessing a series of derivatives from one basic structure.

Ionic liquids own a binary structure with cationic and anionic parts. From previous studies, it is known that the coupling of a cation core with different counterions would afford ionic liquids with totally different properties, such as different micro-environments, diverse molecular interactions, and distinct physicochemical properties. In our case, the influence of the coupled counterion on the energy of the HOMO and LUMO as well as on the band gap (eV) of the PAI cation core was firstly calculated by using density functional theory at the B3LYP/6-31G(d) level.^[15] It was found, as shown in Figure 2 and Table S1 in the Supporting Infor-

mation, that the HOMO and LUMO energies as well as the corresponding band gaps could be greatly changed through the introduction of different counterions. This result implied that the counterion exchange of the synthesized IL sensing element offered a feasible way for effectively tuning its sensing properties.

To experimentally confirm the possibility of creating various sensing elements by a simple exchange of the counterion, the optical properties of the prepared silica films with different counterions were also measured as shown in Figure 3. All emission spectra showed three primary characteristic emission peaks at λ = 345, 360 and 389 nm but obvious differential intensities at each peak. Similarly, although the excitation spectra were clearly divided into three zones: λ = 240–270, 270–308, and 308–360 nm, the PAI core showed different excitation patterns with different anions. Also the induced diversities by coupling different counterions could be found in the aspect of excited-state lifetimes. As shown in Table S2 and Figure S5 in the Supporting Information, all six decay profiles were fitted by tri-exponential decay kinetics to show three nanosecond time domains. However, due to the variation of the counterions, these three time domains in each sample took different percentages.

All results described above proved the feasibility that a simple counterion exchange approach could be exploited for generating receptors or sensor elements with rich diversities. Virtually, ionic liquids offer an unlimited tunability. In addition, based on the concept of “task-specific” ionic liquids, functional groups as anions can also be introduced into IL units, leading to ILs with specific functions. Clearly, these fascinating features may provide an attractive opportunity and assurance for rapidly and efficiently creating a big sensor element pool with rich diversities from one basic IL sensor element.

Construction of a cross-reactive sensor array for nitroaromatics and explosives mimics detection: Rapid detection and discrimination of hidden explosives are very important aspects concerning homeland security as well as environmental and humanitarian safety.^[16] To demonstrate the great potential of the strategy described above in the construction of a cross-reactive sensor array, the sensor elements with five different counterions (Cl⁻, Br⁻, NO₃⁻, Ala⁻, and Gln⁻) produced by a simple counterion exchange of the synthesized fluorescent IL **3** were used as an initial array for the discrimination of six nitroaromatics and explosives mimics (see Scheme 1). In our work, the analyte sensing was done by following the same method described by Swager et al., which was also employed in most of reported work in the explosive detection field. Actually, due to the macro-mesoporous hierarchical structure in our system, the detection limit could be far less than the concentration at the saturated vapor pressure.

The differential sensing capability of each sensor element was evaluated, and the sensing measurement was repeated five times for each analyte. After measurement of their initial fluorescent intensity, each sensor element was exposed

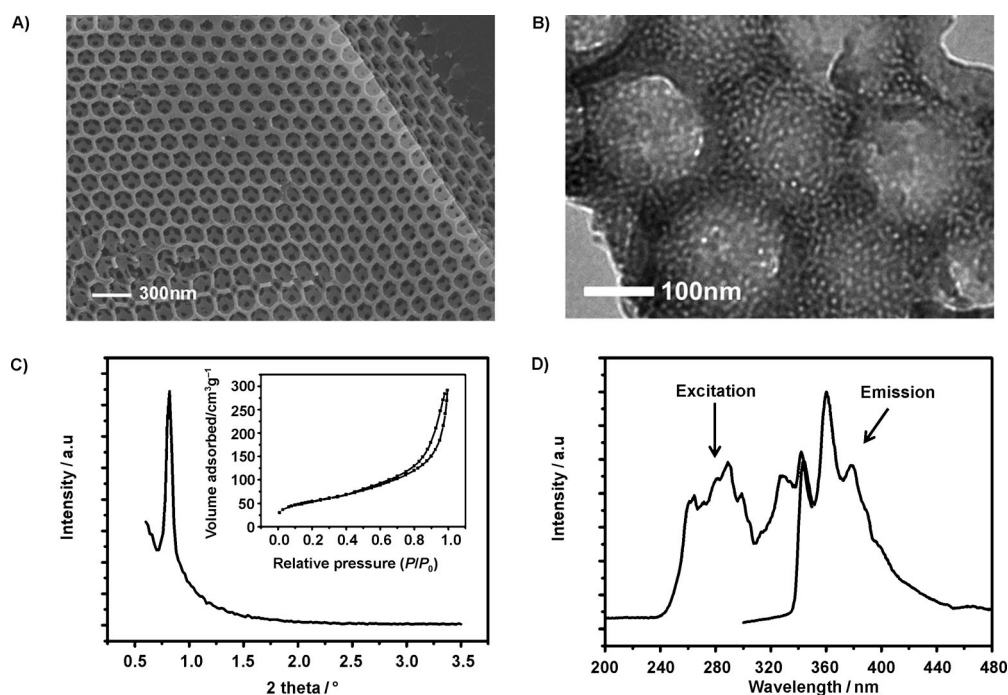


Figure 1. A) SEM (scale bar = 300 nm) and B) TEM (scale bar = 100 nm) images of the IL-doped silica film with a macro-mesoporous structure. C) XRD pattern and N_2 adsorption–desorption isotherms (insert) of the hybrid silica film. D) Fluorescence excitation and emission spectra of the PAI-based ionic liquid molecules in the formed silica film.

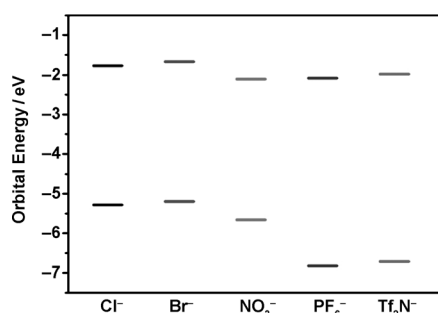


Figure 2. Band gap energies of the fluorescent PAI-based ionic liquid sensor element with different counterions, which were calculated by using density functional theory at the B3LYP/6-31G(d) level for the optimized geometries.

to six different nitroaromatics and explosives mimics, and their fluorescence intensity was scanned again. Figure 4 shows the plot of the change in the fluorescence intensity as a percentage of the original ($((F_0 - F)/F_0)100\%$), which gives each detected analyte a 5D fingerprint. Taking a close comparison in the fingerprints, we found that the nitroaromatics TNT, DNT, and DN have a better quenching efficiency, and the quenching reached 60% in 120 s, which is indicative of a good sensitivity. Furthermore, the best sensing performance for each analyte was irregularly hopping between the sensors in a 5-IL array system. To better illustrate the differential sensing properties of the IL sensor elements, the maximum and minimum quenching efficiencies are displayed in Figure 4F. Clearly, dependent on the coupled counterion, the quenching efficiency of the IL sensor element for each

analyte varied in a wide range, indicating that counterion exchange is a powerful mean for effective adjustment of the sensing properties of the IL sensor element.

The observed recognition patterns of the IL-based sensor array toward six different samples were subjected to a principal component analysis (PCA) to generate a clustering map for more practical visualization. PCA is a non-supervised mathematical method that can transform a number of correlated variables into uncorrelated variables called principal components (PCs).^[5] The first principal component (PC1) contained the highest degree of variance, and the other PCs followed in the order of decreasing variance. In this way, the PCA concentrates the most significant characteristics of the whole data into a lower dimensionally space without losing much information. In Figure 5, the PCA of the data obtained from six samples on a 5-IL sensor array is shown in a 3D-Euclidean space, which contained 98.69% of the information. The 3D-PCA plot contains points for each of the nitrated samples measured five times. The responses for each sample were clustered into six distinct groups, demonstrating a good reproducibility. This result suggests that the initial IL sensor array fabricated with randomly selected counterions, already shows a good detection and discrimination ability for the analytes.

Sensor array with a dynamic tunable feature: The introduction of dynamic adjustability in a sensor array could endow the array a better controllability and practicality. Herein, the dynamic feature focused on the aspects of the properties and sensor capability, and the overall performance of the

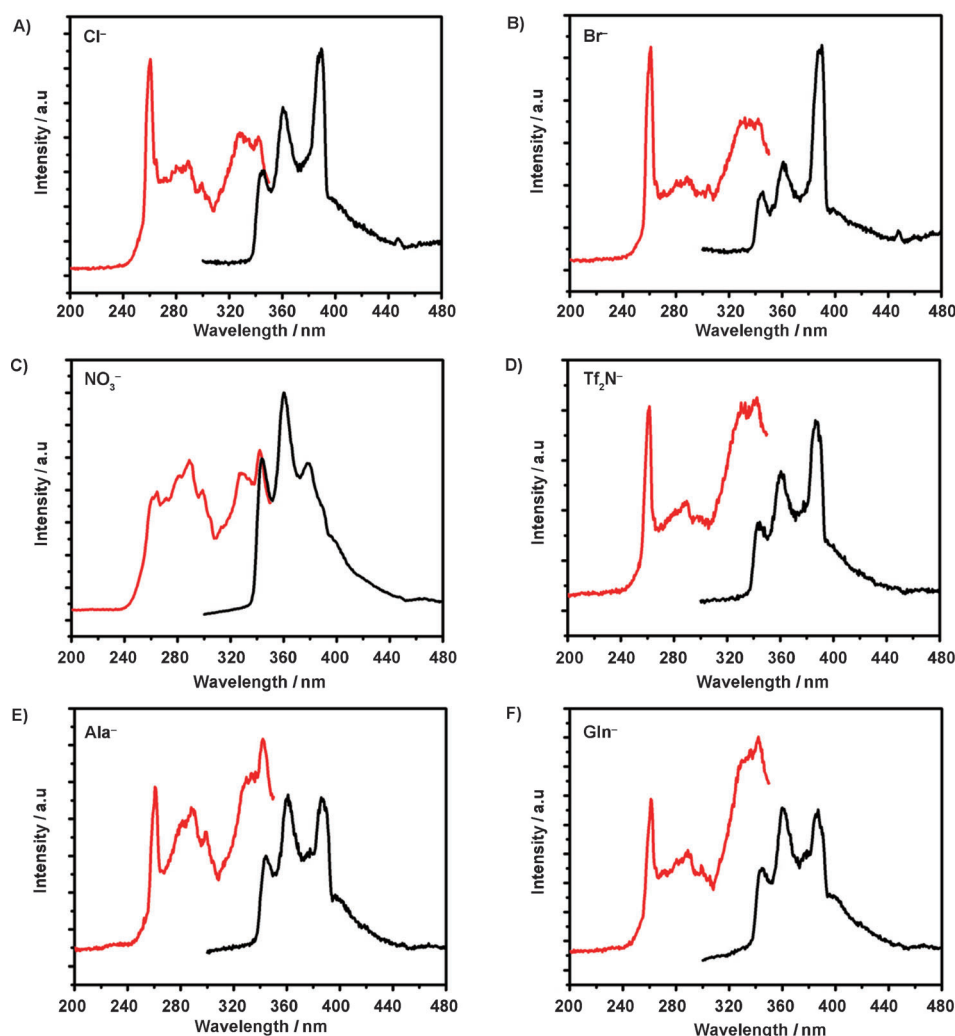


Figure 3. Fluorescence excitation spectra (red line, $\lambda_{Em}=387$ nm) and emission spectra (black line, $\lambda_{Ex}=260$ nm) of the PAI-based ionic liquid sensor element with six different counterions in the formed silica films.

array. In our case, due to the reversible anion exchange ability, it offered the possibility to own this dynamic feature in our ionic-liquid-based arrays.

In the above discussion, we have proven that the individual receptors, which were generated by simple counterion exchange, had different properties. Due to the reversible anion exchange, these properties were dynamically tunable. To further demonstrate the dynamic adjustment in the sensing properties of the sensor element, we explored the time-dependent fluorescence quenching curves upon exposure to saturated dinitrobenzene and 2,4-dinitrotoluene vapors, which are shown in Figure 6. In the case of the IL sensor with Ala^- as counterion, only 28% of the initial fluorescence was quenched by DN after 60 s exposure (Figure 6A). However, the displacement of the counterion with PF_6^- led to a remarkable improvement of the quenching efficiency of the IL sensor. A fluorescence quenching of 56% occurred after 60 s, and 70% quenching was detected after 120 s. A similar phenomenon was also observed for the case of DNT (Figure 6B). Obviously, the displacement of the counterion can

efficiently change the sensing properties of an individual sensor element, providing a desirable and dynamic means to turn the performance of the established sensor array.

As mentioned above, an array with four IL sensor elements (named array 1) was firstly created with randomly selected counterions (Cl^- , Br^- , Ala^- , and Tf_2N^-), which shows a modest detection and discrimination for six nitrated samples, see Figure S6 in the Supporting Information. Based on the simple anion displacement, the arrays 2–4 could be facily derived from the established array 1, as shown in Figure 7. In array 1, the four analytes (TNT, DNT, DN, and CB) clustered in close proximity. Particularly, the data between TNT and DNT had some degree of overlap for hard classification. In array 2, which was produced by replacing Br^- with PF_6^- , no clear improvement of the discrimination was achieved. However, in array 3 the responses for each analyte were clustered into six distinct groups, suggesting a good discrimination. The average Euclidean distance between the three

classes of TNT, DNT, and DN is 0.39. Fortunately, after carefully screening the counterions in array 1, array 4 with a good discrimination was established. The calculated average Euclidean distance between the three classes of TNT, DNT, and DN increased from 0.39 to 0.98. The “jack-knife” analysis showed 100% correct classification in the formed sensor array when all three roots were taken into consideration. These results demonstrate that the dynamic tunable feature in the IL-based sensor arrays is very useful for convenient and efficient optimization or extension of the formed sensor array.

Rational design of an IL-based sensor array: The anion exchange method was a powerful strategy to create a large amount of sensor elements for array construction. However, it was not true that the more sensor elements, the better sensing performance. During the development of array-based detection systems, it had been proven that increasing the number of receptors would increase the overall sensing performance. This was attributed to the increase in the di-

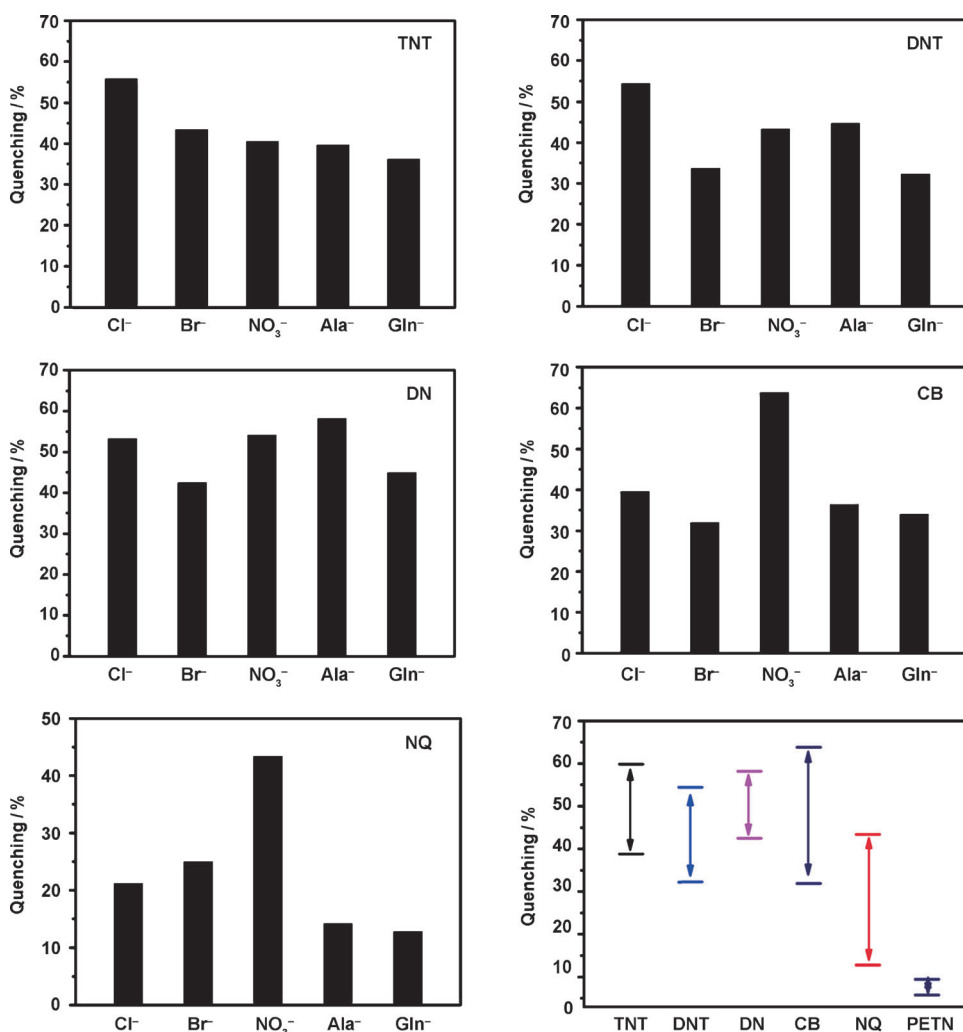


Figure 4. A–E) Fingerprints for the five nitroaromatics and explosives mimics in the five-element of the PAI-based ionic liquid sensor arrays. F) Maximum and minimum fluorescence quenching of the PAI-based ionic liquid sensor elements with five counterions upon exposure to the six analytes.

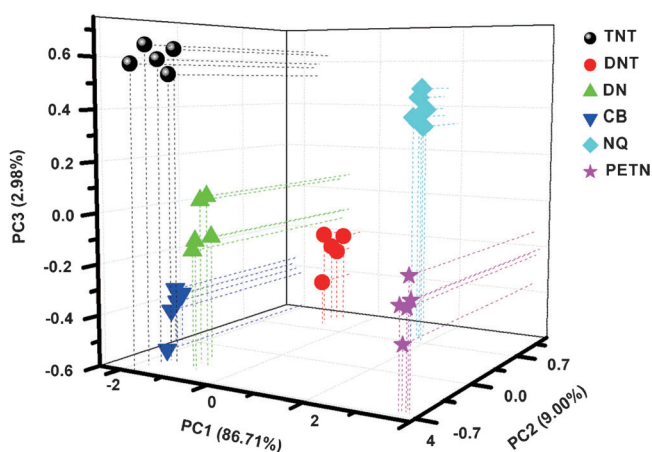


Figure 5. PCA score plot of the three PCs describing approximately 98.7% of the total variance. The PCA score plot shows six clustering for all samples.

versity of receptors, which led to an increase in the responsive information.^[6] However, after a certain point, increasing the number of receptors may lead to a little effect suggesting an optimized number for analyte discrimination.

To demonstrate the similar property in the IL-based sensor array, we first construct a primary array A with seven individual sensor elements. Following the similar data processing method described in the work of Anzenbacher et al.,^[5] arrays B (five elements) and C (four elements) were sequentially derived from the primary array A (Figure 8). During the minimization procedure, the correct classification and good resolving power were the two most concerned factors. With the assistance of LDA and the “jack-knife” analysis based on three roots, all the raw array A as well as the reduced arrays B and C showed 100% correct classification in all 30 cases. Although it was notable that even after excluding the two (S1, S6) or three (S1, S6, S7) out of the raw array A, the PCA score plot in array B and C still showed good clustering with

no evident overlap between the samples. Further comparison of the resolving power of each array was performed only between the arrays B and C for the smaller array size. As shown in Figure 8, the average Euclidean distances between the samples were 2.88 for array B and 2.53 for array C, respectively. The increased ratio was about 14%, indicating that array B had a better discriminatory performance and resolving power. These observations suggest that by optimizing the number and diversity of the receptors in the array, we could really obtain a good resolution array with optimized size.

The results described above were encouraging. Based on the anion exchange approach, a rapid, facile, and efficient way to create a cross-reactive sensor array with dynamic adjustability was realized for the identification and classification of nitroaromatics and explosives mimics. Herein, the anion exchange is the key feature for the IL-based sensor array. In our work, although the hypothesis where different counterions affect the response to different analytes has

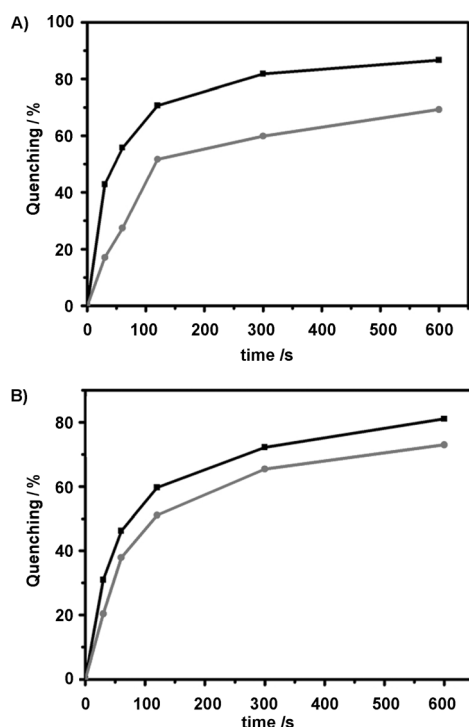


Figure 6. Time-dependent fluorescence quenching of the PAI-based sensor elements with PF_6^- (top curves) and Cl^- (bottom curves) as counterions upon exposure to A) DN and B) DNT.

been proven by a series of experiments, however, the corresponding mechanism at the molecular level is still not clear. In the future we will focus on the investigation of the mechanism both in a theoretical and experimental way to gain deep understanding of this kind of system and thus to afford high-performance sensor array devices. In addition, although a PAI-based luminescent ionic liquid was selected for sensing, actually other types of luminescent ionic liquids with different excitation wavelengths could also be used to broaden the sensor array application. Recently, many ionic liquids had also been found to selectively enrich analytes. For example, in the work of Tao et al., [BMIM] PF_6 (BMIM=1-butyl-3-methylimidazolium) was used for selectively enriching the aromatic explosives.^[16] Thus, this property of ionic liquids would add a new spatial dimension in the IL-based array to further increase the discriminatory performance and resolving power of the sensor array.

Conclusion

In summary, based on the simple counterion exchange of ionic liquid, a rapid, facile and efficient strategy to create cross-reactive sensor array with dynamic tunable feature was developed, and exemplified by the construction of sensor array for six nitroaromatics and explosives mimics identification and classification. It was found that the LUMO-HOMO energies, excitation and emission spectra, fluorescent lifetimes as well as the sensing capability of the

synthesized IL could be significantly influenced and tuned by coupling different counteranions, indicating that from one single IL sensor element a big sensor element pool with rich diversities could be conceivably created by simple exchange process of counteranions. Moreover, the reversible counterion exchange capability of IL also provides a huge room and useful means to post-modify the sensing properties of individual element for further correcting or optimizing the sensing performance of the formed sensor array, and so endows the array with desirable dynamic tunable feature. With the assistance of statistical analysis such as principal component analysis (PCA) and linear discrimination analysis (LDA), an optimized-size array with high resolution can be rationally established from a large number of the IL-based receptors. Although PAI-based luminescent ionic liquid was used for present study, these results are expected to be universal for other types of ionic liquids. In addition, based on the concept of “task-specific” ionic liquids, functional groups as anions can also be introduced into IL units, leading to ILs with specific functions. Thus, we believed our developed strategy offered a powerful method for facilely and efficiently constructing sensor array, which could find a wide range of applications.

Experimental Section

The general methods used for compound identification as well as purchase information are given in the Supporting Information.

Synthesis of 1*H*-phenanthro[9,10-*d*]imidazole (1): 9,10-Phenanthrenequinone (5.0 g, 0.024 mol) was dissolved in formaldehyde (3.85 mL, 37 wt %) containing glacial acetic acid (93.33 mL, 1.63 mol) and ammonium acetate (38.45 g, 0.5 mol). The resulting reaction mixture was heated to reflux for 4 h. After cooling, the reaction mixture was diluted with water (100 mL) and neutralized with concentrated aqueous ammonia (30 wt %) to pH 7 to get a light cream precipitate. After filtering, the obtained solid was washed with water, acetone, dichloromethane, and ethyl ether, and then dried to afford the desired product. $^1\text{H NMR}$ (400 MHz, $[\text{D}_6]\text{DMSO}$): δ =8.85 (d, J =8 Hz, 2H; Ar-H), 8.55–8.35 (m, 3H; NH, Ar-H), 8.32 (s, 1H; N=CH), 7.70 (t, J =14 Hz, 2H; Ar-H), 7.62 ppm (t, J =14 Hz, 2H; Ar-H); MS (ESI+): m/z : 437.2 $[2M+H]^+$.

Synthesis of 1-butylphenanthro[9,10-*d*]imidazole (2): Compound 1 (4.0 g, 18.4 mmol) and sodium hydroxide (0.8 g, 20 mmol) were resolved in DMSO (40 mL). The reaction mixture was stirred at room temperature for 2 h. After addition of butyl bromide (2.0 mL, 18.4 mmol), the reaction solution was stirred at room temperature for further 25 min, then the temperature was increased to 37°C. After overnight reaction under stirring, the solvent was removed and the residue was taken up in acetonitrile (30 mL). After filtration, the solvent was removed and the residue was further purified by trituration with ethyl ether to give the desired product. $^1\text{H NMR}$ (400 MHz, $[\text{D}_6]\text{DMSO}$): δ =8.94 (d, J =9 Hz, 1H; Ar-H), 8.85 (d, J =9 Hz, 1H; Ar-H), 8.53 (d, J =9 Hz, 1H; Ar-H), 8.35 (d, J =9 Hz, 1H; Ar-H), 8.26 (s, 1H; N=CH), 7.80–7.60 (m, 4H; Ar-H), 4.71 (t, J =7 Hz, 2H; N- CH_2), 1.93–1.83 (m, 2H; N CH_2CH_2), 1.40–1.30 (m, 2H; CH_2CH_3), 0.92 ppm (t, J =9 Hz, 3H; CH_3); MS (ESI+): m/z : 275.2 $[M+H]^+$.

Synthesis of 1-butyl-3-(3-trimethoxysilyl)propyl)phenanthro[9,10-*d*]imidazol-3-ium iodide (3): Compound 2 (0.5 g, 1.8 mmol) and (3-iodopropyl)-trimethoxysilane (2.4 g, 8.3 mmol) were added into a pressure flask. The flask was vacuumed, and the reaction mixture was stirred at 100°C for 48 h. After removal of unreacted (3-iodopropyl)trimethoxysilane, the red pure product was obtained. $^1\text{H NMR}$ (300 MHz, $[\text{D}_6]\text{DMSO}$): δ =

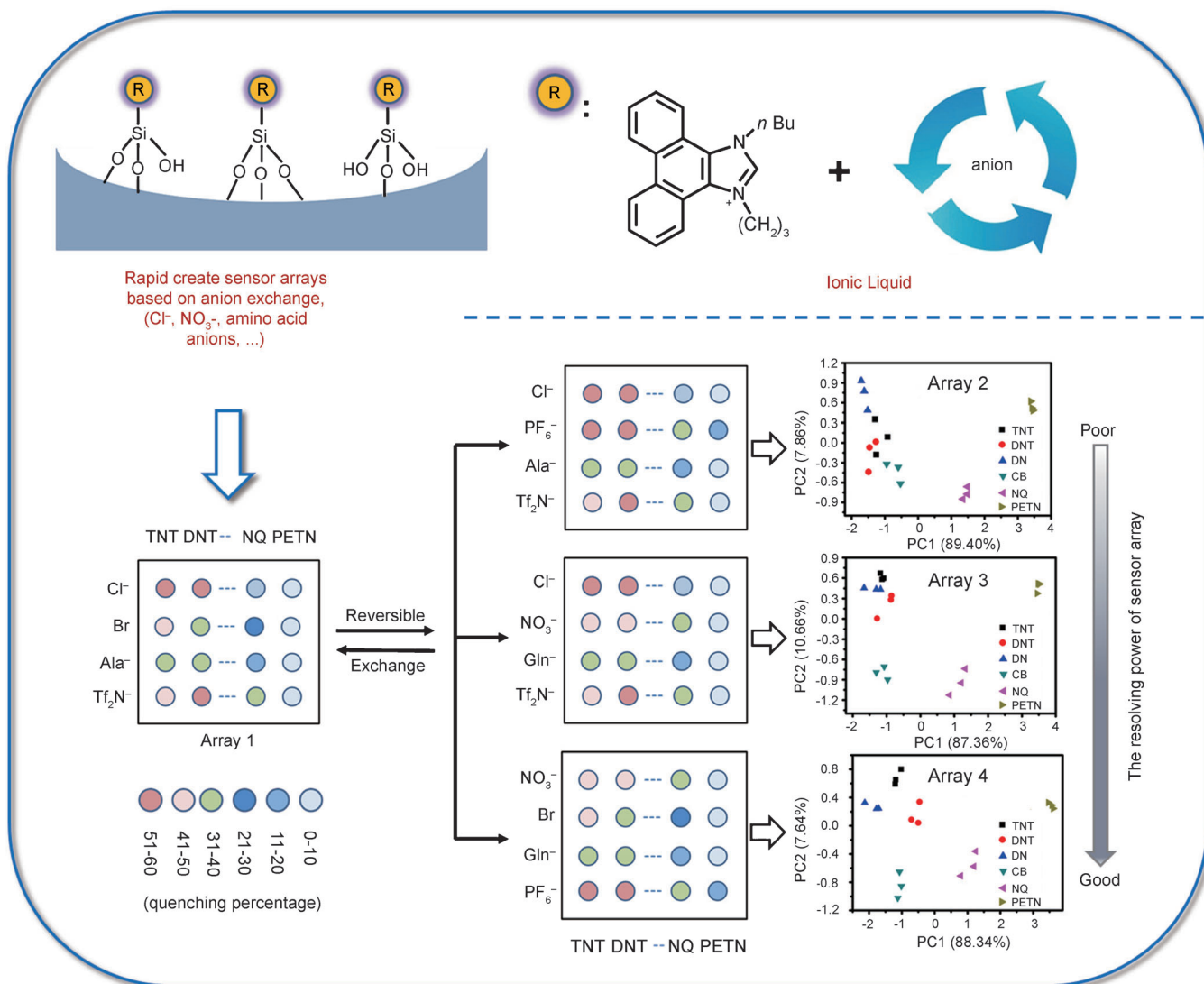


Figure 7. Schematic illustration of the reversible anion exchange process to demonstrate the dynamic tunable feature of the ionic-liquid-based sensor arrays. Array 1 is firstly created with four randomly selected counterions (Cl⁻, Br⁻, Ala⁻, and Tf₂N⁻). Arrays 2–4 are further facilely derived from the established array 1 by simple anion displacement. PCA and LDA are used for statistical analysis. Among these four arrays, array 4 has the best accuracy and resolving power. ■ = TNT, ● = DNT, ▲ = DN, ▼ = CB, ◀ = NQ, ▶ = PETN.

9.79 (s, 1H; N-CH), 9.10 (d, $J=8.7$ Hz, 2H; Ar-H), 8.54 (d, $J=6.9$ Hz, 2H; Ar-H), 7.95–7.85 (m, 4H; Ar-H), 4.95–4.85 (m, 4H; N-CH₂), 3.46 (s, 6H; OCH₃), 2.07–1.99 (m, 4H; NCH₂CH₃), 1.43–1.53 (m, 2H; CH₂CH₃), 0.97 (t, $J=6.7$ Hz, 3H; CH₃), 0.83–0.66 ppm (m, 2H; Si-CH₂); MS (ESI⁺): m/z : 437.3 [M-1]⁺.

Formation of the ionic-liquid-doped silica films with macro-mesopore structure: The PAI-bridged silane **3** (50 mg, 8.86×10^{-2} mmol), tetraethyl orthosilicate (TEOS) (1.04 g, 5 mmol), and ethanol (5.82 g) were dissolved in water (0.73 g, 41 mmol) containing 1 M HCl (105 μ L), and the resulting reaction mixture was heated to reflux at 60 °C for 30 min. Then, surfactant F127 (0.26 g) and anhydrous ethanol (5.82 g) were added for further 30 min stirring. The final molar ratio of the reactants was 1 TEOS/PAI/EtOH/H₂O/HCl/F127 = $1:1.78 \times 10^{-2}:50.6:9.28:2.1 \times 10^{-2}:4.12 \times 10^{-3}$. Then the synthesized precursor was infiltrated into PS colloidal crystal voids until they became transparent. To increase the stability of the formed porous framework, the obtained films were aged in oven (60 °C) for eight days. Finally, the used templates (PS spheres and F127)

were extracted by toluene and ethanol to form the PAI-functionalized silica films with macro-mesoporous structure.

Anion exchange procedure: The synthesized silica films were soaked into 0.2 M aqueous solutions of the corresponding salt, such as NaCl, NaBr, NaNO₃, NaPF₆, LiTf₂N, NaAla, and NaGln. After 2 h anion exchange reaction, the films were washed thoroughly with water and dried in air. Before the sensing experiments, all the prepared films were vacuumed at 80 °C for 2 h.

Acknowledgements

We gratefully acknowledge financial support from the National Science Foundation of China (No. 50873051, 205333050, 21273284), MOST (2007AA03Z307), and Transregional Project (TRR61).

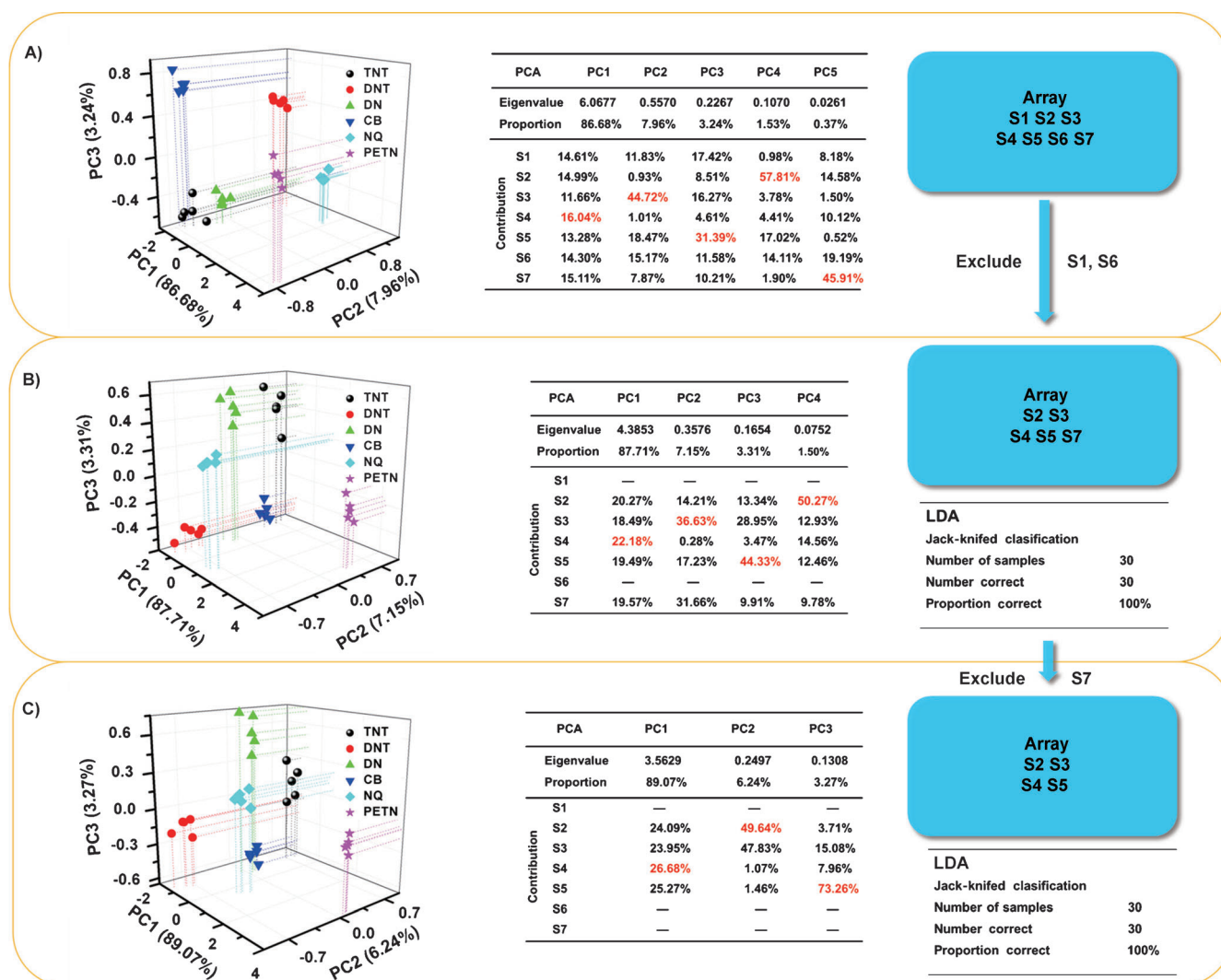


Figure 8. Schematic illustration of the rational process for optimizing the number of sensor elements in an array. A) PCA for all sensors (S1–S7) shows that the main contributors for the dispersion are S2–S5, and S7 on the PCs. B) Sensor elements S1 and S6 are excluded for an analysis again with PCA. PCA shows that the main contributors are S2–S5. C) S7 is excluded and PCA is used for further statistical analysis. Cross-validated LDA shows that all the sensor arrays A–C have a 100% accurate classification.

- [1] a) K. J. Albert, N. S. Lewis, C. L. Schauer, G. A. Sotzing, S. E. Stitzel, T. P. Vaid, D. R. Walt, *Chem. Rev.* **2000**, *100*, 2595–2626; b) F. Röck, N. Barsan, U. Weimar, *Chem. Rev.* **2008**, *108*, 705–725.
- [2] a) T. A. Dickinson, J. S. White, J. S. Kauer, D. R. Walt, *Nature* **1996**, *382*, 697–700; b) M. N. Stojanovic, E. G. Green, S. Semova, D. B. Nikic, D. W. Landry, *J. Am. Chem. Soc.* **2003**, *125*, 6085–6089; c) E. Green, M. J. Olah, T. Abramova, L. R. Williams, D. Stefanovic, T. Worgall, M. N. Stojanovic, *J. Am. Chem. Soc.* **2006**, *128*, 15278–15282; d) A. Duarte, A. Chworos, S. F. Flagan, G. Hanrahan, G. C. Bazan, *J. Am. Chem. Soc.* **2010**, *132*, 12562–12564; e) L. D. Bonifacio, D. P. Puzzo, S. Breslav, B. M. Wiley, A. McGree, G. A. Ozin, *Adv. Mater.* **2010**, *22*, 1351–1354; f) F. Samain, S. Ghosh, Y. N. Teo, E. T. Kool, *Angew. Chem.* **2010**, *122*, 7179–7183; *Angew. Chem. Int. Ed.* **2010**, *49*, 7025–7029; g) S. S. Tan, S. J. Kim, E. T. Kool, *J. Am. Chem. Soc.* **2011**, *133*, 2664–2671; h) M. E. Germain, M. J. Knapp, *J. Am. Chem. Soc.* **2008**, *130*, 5422–5423; i) Y. L. Liu, M. A. Palacios, P. Anzenbacher, Jr., *Chem. Commun.* **2010**, *46*, 1860–1862.
- [3] a) S. C. McCleskey, M. J. Griffin, S. E. Schneider, J. T. McDevitt, E. V. Anslyn, *J. Am. Chem. Soc.* **2003**, *125*, 1114–1115; b) A. T. Wright, M. J. Griffin, Z. L. Zhong, S. C. McCleskey, E. V. Anslyn, J. T. McDevitt, *Angew. Chem.* **2005**, *117*, 6533–6536; *Angew. Chem. Int. Ed.* **2005**, *44*, 6375–6378; *Angew. Chem.* **2005**, *117*, 6533–6536; c) A. T. Wright, E. V. Anslyn, J. T. McDevitt, *J. Am. Chem. Soc.* **2005**, *127*, 17405–17411; d) T. Zhang, N. Y. Edwards, M. Bonizzoni, E. V. Anslyn, *J. Am. Chem. Soc.* **2009**, *131*, 11976–11984.
- [4] a) N. T. Greene, S. T. Morgan, K. D. Shimizu, *Chem. Commun.* **2004**, 1172–1173; b) N. T. Greene, K. D. Shimizu, *J. Am. Chem. Soc.* **2005**, *127*, 5695–5700.
- [5] a) M. A. Palacios, Z. Wang, V. A. Montes, G. V. Zyryanov, P. Anzenbacher, Jr., *J. Am. Chem. Soc.* **2008**, *130*, 10307–10314; b) M. A. Palacios, R. Nishiyabu, M. Marquez, P. Anzenbacher, Jr., *J. Am. Chem. Soc.* **2007**, *129*, 7538–7544; c) G. V. Zyryanov, M. A. Palacios, P. Anzenbacher, Jr., *Angew. Chem.* **2007**, *119*, 7995–7998; *Angew. Chem. Int. Ed.* **2007**, *46*, 7849–7852; *Angew. Chem.* **2007**, *119*, 7995–7998.
- [6] a) U. H. F. Bunz, V. M. Rotello, *Angew. Chem.* **2010**, *122*, 3338–3350; *Angew. Chem. Int. Ed.* **2010**, *49*, 3268–3279; b) C. C. You, O. R. Miranda, B. Gider, P. S. Ghosh, I. B. Kim, B. Erdogan, S. A. Kroví, U. H. F. Bunz, V. M. Rotello, *Nat. Nanotechnol.* **2007**, *2*, 318–323; c) M. De, S. Rana, H. Akpinar, O. R. Miranda, R. R. Arvizo, U. H. F. Bunz, V. M. Rotello, *Nat. Chem.* **2009**, *1*, 461–465; d) L.

- Baldini, A. J. Wilson, J. Hong, A. D. Hamilton, *J. Am. Chem. Soc.* **2004**, *126*, 5656–5657; e) H. Zhou, L. Baldini, J. Hong, A. J. Wilson, A. D. Hamilton, *J. Am. Chem. Soc.* **2006**, *128*, 2421–2425; f) D. Margulies, A. D. Hamilton, *Angew. Chem.* **2009**, *121*, 1803–1806; *Angew. Chem. Int. Ed.* **2009**, *48*, 1771–1774.
- [7] a) A. Buryak, K. Severin, *Angew. Chem.* **2004**, *116*, 4875–4878; *Angew. Chem. Int. Ed.* **2004**, *43*, 4771–4774; b) A. Buryak, K. Severin, *J. Am. Chem. Soc.* **2005**, *127*, 3700–3701; c) A. Buryak, K. Severin, *Angew. Chem.* **2005**, *117*, 8149–8152; *Angew. Chem. Int. Ed.* **2005**, *44*, 7935–7938.
- [8] a) S. H. Lim, L. Feng, J. W. Kemling, C. J. Musto, K. S. Suslick, *Nat. Chem.* **2009**, *1*, 562–567; b) N. A. Rakow, K. S. Suslick, *Nature* **2000**, *406*, 710–713; c) C. Zhang, K. S. Suslick, *J. Am. Chem. Soc.* **2005**, *127*, 11548–11549.
- [9] A. P. Umali, E. V. Anslyn, *Curr. Opin. Chem. Biol.* **2010**, *14*, 685–692.
- [10] H. S. Hewage, E. V. Anslyn, *J. Am. Chem. Soc.* **2009**, *131*, 13099–13106.
- [11] N. V. Plechkova, K. R. Seddon, *Chem. Soc. Rev.* **2008**, *37*, 123–150.
- [12] E. Borzin, A. Shemesh, C. H. Ronen, Y. Gerchikov, N. Tessler, Y. Eichen, *J. Phys. Org. Chem.* **2010**, *23*, 1108–1113.
- [13] a) X. X. Jin, L. Yu, D. Garcia, R. X. Ren, X. Q. Zeng, *Anal. Chem.* **2006**, *78*, 6980–6989; b) K. Y. Hou, A. Rehman, X. Q. Zeng, *Langmuir* **2011**, *27*, 5136–5146; c) C. H. Xiao, A. Rehman, X. Q. Zeng, *Anal. Chem.* **2012**, *84*, 1416–1424.
- [14] a) A. Stein, F. Li, N. R. Denny, *Chem. Mater.* **2008**, *20*, 649–666; b) F. Li, Z. Y. Wang, N. S. Ergang, C. A. Fyfe, A. Stein, *Langmuir* **2007**, *23*, 3996–4004; c) Z. Y. Yuan, B. L. Su, *J. Mater. Chem.* **2006**, *16*, 663–677; d) M. Antonietti, G. A. Ozin, *Chem. Eur. J.* **2004**, *10*, 28–41.
- [15] a) A. D. Becke, *J. Chem. Phys.* **1993**, *98*, 5648; b) C. Lee, W. Yang, R. G. Parr, *Phys. Rev. B* **1988**, *37*, 785.
- [16] a) S. W. Thomas, G. D. Joly, T. M. Swager, *Chem. Rev.* **2007**, *107*, 1339–1386; b) D. T. McQuade, A. E. Pullen, T. M. Swager, *Chem. Rev.* **2000**, *100*, 2537–2574; c) J. C. Sanchez, W. C. Trogler, *J. Mater. Chem.* **2008**, *18*, 3143–3156; d) M. E. Germain, M. J. Knapp, *Chem. Soc. Rev.* **2009**, *38*, 2543–2555; e) T. Naddo, Y. K. Che, W. Zhang, K. Balakrishnan, X. M. Yang, M. Yen, J. C. Zhao, J. S. Moore, L. Zang, *J. Am. Chem. Soc.* **2007**, *129*, 6978–6979; f) Y. Salinas, R. M. Máñez, M. D. Macos, F. Sancenón, A. M. Costero, M. Parra, S. Gil, *Chem. Soc. Rev.* **2012**, *41*, 1261–1296; g) A. Ponnuru, N. Y. Edwards, E. V. Anslyn, *New J. Chem.* **2008**, *32*, 848–855; h) A. D. Hughes, I. C. Glenn, A. D. Patrick, A. Ellington, E. V. Anslyn, *Chem. Eur. J.* **2008**, *14*, 1822–1827.
- [17] E. S. Forzani, D. L. Lu, M. J. Leright, A. D. Aguilar, F. Tsow, R. A. Lglesias, Q. Zhang, J. Lu, J. H. Li, N. J. Tao, *J. Am. Chem. Soc.* **2009**, *131*, 1390–1391.

Received: February 28, 2013
Published online: July 19, 2013